The Journal of Experimental Biology 213, 3340-3347

doi:10.1242/jeb.046862

Angiogenesis of the uterus and chorioallantois in the eastern water skink *Eulamprus quoyii*

Bridget F. Murphy[1,*], Scott L. Parker[2], Christopher R. Murphy[3] and Michael B. Thompson[1]

[1]Integrative Physiology Research Group, School of Biological Sciences, University of Sydney, Sydney, NSW 2006, Australia, [2]Department of Biology, Coastal Carolina University, Conway, SC 25926, USA and [3]Discipline of Anatomy and Histology, School of Medical Science and Bosch Institute, The University of Sydney, Sydney, NSW 2006, Australia

*Author for correspondence (bridget.murphy@sydney.edu.au)

Accepted 31 June 2010

SUMMARY

We have discovered a modification of the uterus that appears to facilitate maternal-fetal communication during pregnancy in the scincid lizard *Eulamprus quoyii*. A vessel-dense elliptical area (VDE) on the mesometrial side of the uterus expands as the embryo grows, providing a large vascular area for physiological exchange between mother and embryo. The VDE is already developed in females with newly ovulated eggs, and is situated directly adjacent to the chorioallantois of the embryo when it develops. It is likely that signals from the early developing embryo determine the position of the VDE, as the VDE is off-centre in cases where the embryo sits obliquely in the uterus. The VDE is not a modification of the uterus over the entire chorioallantoic placenta, as the VDE is smaller than the chorioallantois after embryonic stage 33, but expansion of the VDE and growth of the chorioallantois during pregnancy are strongly correlated. The expansion of the VDE is also strongly correlated with embryonic growth and increasing embryonic oxygen demand ($\dot{V}_{O_2}$). We propose that angiogenic stimuli are exchanged between the VDE and the chorioallantois in *E. quoyii*, allowing the simultaneous growth of both tissues.

Key words: lizard, viviparity, uterus, angiogenesis, embryo, *Eulamprus quoyii*.

INTRODUCTION

Viviparity is the retention of the embryo *in utero* until it is fully developed; during gestation, fetal membranes and maternal uterine tissues are in intimate contact (Guillette and Jones, 1985). If viviparity evolves as a gradual increase in the duration of egg retention in oviparous species (Packard et al., 1977; Shine, 1983; Shine, 1985), then the uterus must develop the capacity to support the metabolic demands of the embryo during such a prolonged period *in utero* (Parker and Andrews, 2006; Parker et al., 2010a). As the embryo and its extra-embryonic membranes grow and differentiate during pregnancy, changes in vascular density occur in the surrounding uterine tissue to support embryonic growth (Guillette and Jones, 1985; Parker et al., 2010a; Parker et al., 2010b).

The intimate association of the uterus with the chorioallantois, the extra-embryonic membrane involved in respiratory gas exchange, is called the chorioallantoic placenta. The diverse patterns of chorioallantoic placentation in viviparous lizards (Weekes, 1935; Blackburn and Vitt, 2002) provide an ideal model in which to study the physiological triggers of uterine vascularization (angiogenesis). Although the triggers of uterine angiogenesis in lizards are unknown, one potential physiological stimulus is hypoxic conditions *in utero* (Guillette and Jones, 1985). Rapid uterine angiogenesis coincides with the 'exponential' growth phase of the embryo and a highly vascular uterus might be required to maintain sufficiently high partial pressures of oxygen to allow embryonic development to continue (Guillette and Jones, 1985; Masson and Guillette, 1987; Parker et al., 2010a). Uterine angiogenesis during pregnancy correlates with embryonic growth in the viviparous skink *Saiphos equalis*, suggesting that uterine angiogenesis might be a response to increasing embryonic metabolism (Parker et al., 2010a). Another potential precursor of uterine angiogenesis is the high concentrations of estrogen and progesterone in the maternal circulation during pregnancy (Yaron, 1972; Fawcett, 1975; Guillette and Jones, 1985). In highly placentotrophic species, such as those of the genus *Mabuya* (Blackburn et al., 1984; Vitt and Blackburn, 1991), embryonic nutrient demand might be the stimulus for the growth of uterine blood vessels (Arany et al., 2008).

Accurate quantitative measurements of uterine vascularity throughout embryonic development are required to determine correlations between uterine vascularity and potential physiological triggers of uterine angiogenesis. Immunofluorescence confocal microscopy of whole-mount preparations of the uterus (Parker et al., 2010a) provides information about uterine vasculature that histology alone cannot. This technique allows the visualization of vasculature across the whole uterus using three-dimensional images, and provides quantitative estimates not only of vessel density and diameter, but also of vessel-length density, a measure of vessel length per unit area.

In this study, we quantified embryonic mass and metabolism, and the vasculature of the uterus and chorioallantois, in the viviparous eastern water skink *Eulamprus quoyii*. *Eulamprus quoyii* is a medium-sized lecithotrophic (Thompson, 1981) viviparous skink with a clutch size of up to nine embryos (personal observation). The placental morphology of this species was originally described using histological techniques (Weekes, 1927). *Eulamprus quoyii* was subsequently included as a representative of a simple Type I chorioallantoic placenta in Weekes's classification scheme (Weekes, 1935). According to Weekes's classification scheme, a Type I placenta consists of a squamous uterine epithelium adjacent to a squamous chorionic epithelium, with any 'modification of maternal and embryonic tissues occurring over the entire area embraced by the allantois' (Weekes, 1935). Our preliminary observations

discovered a thickening of the uterine wall at the mesometrial pole of the uterus in the shape of an ellipse, a structure that is not visible in Weekes's original illustrations. This densely vascularized ellipse is absent in non-reproductive uteri, is present in uteri containing newly-ovulated embryos (<stage 25) (Dufaure and Hubert, 1961), and remains present during pregnancy. We refer to this structure in our descriptions as the vessel-dense ellipse (VDE). We suspect that angiogenesis in the VDE is associated with physiological signals from the embryo and the chorioallantois. If this is the case, then the expansion of the chorioallantois during development should be accompanied by either an increase in the vascular density of the VDE or an increase in the area of VDE.

We used confocal immunofluorescence microscopy to describe and quantify vasculature in pregnant *E. quoyii* in the VDE, on the abembryonic side of the uterus, and in the chorioallantois. We address the following questions. (1) Does the vascular density or the area of the VDE in *E. quoyii* increase during pregnancy? (2) Is the position and the growth of the VDE associated with the position and growth of the chorioallantois? (3) Does uterine angiogenesis occur in concert with embryonic growth and increases in embryonic oxygen demand?

MATERIALS AND METHODS

Animal collection and husbandry

Pregnant *E. quoyii* were collected between October and December in 2008 and 2009 from locations in southern Sydney, Australia. Lizards were housed individually until the end of December in 450 mm × 250 mm × 250 mm aquaria lined with newspaper. Flat rocks were provided for basking and shelter, and lizards were fed approximately five crickets dusted in calcium gluconate every two days. A large water dish supplied water *ad libitum* and 12:12 photophase:scotophase was provided.

Tissue and embryo harvest

Pregnant lizards were killed by decapitation and pithing during a five-week period beginning the last week of October. Lizards were dissected and each uterus containing embryos was removed and floated in a Petri dish of reptile Ringers solution (Frye, 1973). Depending on litter size, one or two embryos from each female were allocated for respirometry measurements, and one or two embryos and the surrounding uterus were fixed for 24 h in 10% neutral-buffered formalin and stored in 70% ethanol for immunohistochemistry.

Embryonic respirometry

Embryos were carefully removed from each uterus, keeping the extra-embryonic membranes intact. Rates of embryonic oxygen consumption ($\dot{V}_{O_2}$) during development were measured at 30°C using closed system respirometry (DeMarco and Guillette, 1992). Volumes of respirometry chambers (468±0.6 ml) were measured to 0.1 ml as described by Thompson and Stewart (Thompson and Stewart, 1997). Chambers were allowed to equilibrate to 30°C for at least two hours before use. Intact embryos were placed into glass cup-shape receptacles and placed in respirometry chambers using a small piece of aluminium foil to support the receptacle. Mass of the embryo, receptacle and foil were measured to 1 mg. Embryos were placed in the chambers together with 0.1 ml of water to humidify the chamber air. Chambers were then sealed and replaced in an incubator at 30°C. After a measured time (range 6–24 h, depending on the rate of oxygen consumption), a gas sample was taken from each chamber into a syringe *via* a three-way stop-cock (Thompson and Stewart, 1997). Samples were injected into one channel of an oxygen analyzer (FC-2 Oxzilla II, Sable Systems, Las Vegas, NV, USA) after passing through Drierite, Ascarite and more Drierite. Two Intelligent Subsamplers (TR-SS3, Sable Systems) were used to draw gas through the oxygen analyzer at approximately 3 ml min^{-1} to achieve a steady reading. Room air (20.94% O_2), scrubbed with Drierite and Ascarite and drawn through the second channel of the analyzer, was used to calibrate the analyzer daily. Output from the oxygen analyzer was recorded using a UI-2 data acquisition interface and ExpeData software (Sable Systems). Barometric pressure was recorded daily from a wall-mounted barometer. $\dot{V}_{O_2}$ was calculated using the equations of Vleck (Vleck, 1987).

Once gas samples had been drawn from each chamber, embryos were examined under a dissecting microscope. Only oxygen consumption measurements from embryos that were healthy and had no visible damage to extra-embryonic membranes were used for data analysis. A strong heart beat in early-stage embryos (stages 30–35), and body movements by later-stage embryos when placed under a light source or gently prodded with a blunt probe (stages 36–40), were used to indicate that embryos were healthy after their time in the respirometry chamber. Respirometry measurements of embryos earlier than stage 30 were omitted from analyses, as strength of the heartbeat in very early embryos was difficult to visibly assess. Embryos were then dissected free of their yolk sac and embryonic stage was determined under the dissecting microscope (Dufaure and Hubert, 1961). Embryos and extra-embryonic membranes were weighed to 1 mg to obtain a measurement of embryo wet mass. Embryos and extra-embryonic membranes were then freeze dried and weighed to 0.01 mg to obtain a measurement of embryo dry mass. In cases where more than one embryo was used from a single female, measurements of oxygen consumption, embryo wet mass and embryo dry mass were averaged.

Immunofluorescence confocal microscopy

Vasculature of the uterus and chorioallantois was visualized using immunofluorescence confocal microscopy on whole-mount preparations, as described by Parker et al. (Parker et al., 2010a). Stacks of images were obtained using a Zeiss LSM 510 Meta confocal microscope (Carl Zeiss, Australia) with 488 nm laser excitation, a 525–555 nm emission filter, a 10× lens and a 0.88×0.88 μm pixel size.

There is a distinctive elliptical vessel-dense region at the mesometrial pole of the uterus in *E. quoyii* (personal observation), the boundary of which is well-defined and visible with the confocal microscope. Images of at least three fields of view (900×900 μm) were captured from both the vessel-dense ellipse (VDE) and the abembryonic hemisphere of the uterus, and from the chorioallantoic membrane (Parker et al., 2010a). Image stacks were flattened to produce 2-dimensional projections of uterine and chorioallantoic vasculature. Indices of vessel-length density (L_V) (mm per mm^2) and vessel density (N_V) (number of vessels per mm^2) were measured as previously described (Parker et al., 2010a). Average vessel diameter (D_V) was calculated by measuring diameters of 30 vessels along a randomly selected transect across each image from the VDE, the abembryonic hemisphere of the uterus and the chorioallantois (Image J, National Institutes of Health, Bethesda, MD, USA).

Using the motorized stage and the 'mark and find' capability of the Zeiss LSM 510 Meta, we measured the width of the VDE in the uterus at its widest point. For each whole-mount preparation, the dorsal uterine artery was used as a central reference point from which distances were measured to the edge of the VDE.

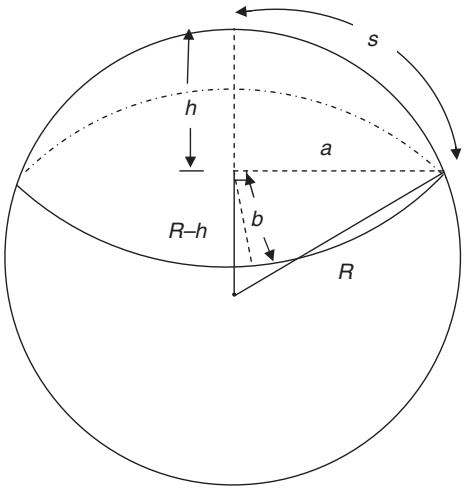

Fig. 1. The formula for the area of a spherical cap is π (a^2+h^2). In the case of a sphere, both radii of the cross section of the cap are the same (a=b). In the case of an ellipse, one radius of the cross section of the cap is longer than the other (b>a). Therefore, we have modified the equation for the area of a spherical cap to estimate the area of an elliptical cap: π (ab+h^2).

Estimations of surface area

The length and average breadth of formalin-fixed eggs (embryos with extra-embryonic membranes and yolk intact) was used to estimate the total egg surface area (Hoyt et al., 1976). The area of the chorioallantois was calculated by multiplying the total egg surface area by an estimate of the percentage of the egg covered by the chorioallantois. To estimate the area of the VDE at the embryonic side of the uterus, we assumed its shape was most similar to an elliptical cap (Fig. 1). The equation for the surface area of a spherical cap (Harris and Stocker, 1998) is:

$$SA_{\text{spherical cap}} = \pi\,(a^2 + h^2)\,, \quad (1)$$

where a is the radius and h is the perpendicular height of the cap (Fig. 1). Because the cross section of a spherical cap is a circle, radius a will equal radius b (Fig. 1). We have modified this equation for a spherical cap to estimate the area of an elliptical cap by assuming that radius b will be longer than radius a in the same ratio that egg length is longer than egg breadth. With this assumption, the equation for the surface area of an elliptical cap becomes:

$$SA_{\text{elliptical cap}} = \pi\,(ab + h^2)\,. \quad (2)$$

Egg diameter was halved to calculate radius R. Width of the VDE was halved to calculate s, the arc length of the circular sector of the egg that defines the elliptical cap. Trigonometry was then used to calculate values of h and a for each egg (Fig. 1). Values for b were calculated by multiplying a by the ratio of egg length:egg breadth for each egg. Changes in the area of the VDE might occur due to stretching of the uterus as the embryo increases in size. Therefore, we also calculated the proportion of the uterine egg chamber covered by the VDE.

Statistical analyses

Embryonic development in viviparous lizards is usually described using a staging system (e.g. Dufaure and Hubert, 1961), but this is not a continuous measure of development as embryos spend progressively more time in each developmental stage as pregnancy proceeds (DeMarco, 1993). Embryo stage as a function of total embryo development time (%TEDT) has been calculated for three species of *Sceloporus* (DeMarco, 1993), where TEDT is the number of days from ovulation to either hatching or parturition. The quadratic relationship between embryo stage and %TEDT was almost identical for all three species of *Sceloporus*, and we have used this equation to convert embryo stages in *E. quoyii* to %TEDT to provide an estimate of embryo development in terms of time.

All analyses are based on mean values (±s.e.m.) for each litter. Q-Q plots were used to confirm normal distributions and Levene's test was used to test homogeneity of variances. SPSS version 17 (SPSS, Chicago, IL, USA) software was used for all statistical analyses and P-values less than 0.05 were considered significant unless otherwise stated. Linear regressions and log–log transformed data were used to determine the rate of embryo growth and increases in metabolism during development (Andrews, 2007). Linear regressions were also used to calculate intra-specific metabolic scaling factors for wet and dry embryos. Linear regressions with a Bonferroni correction were used to test whether the variables L_V, N_V and D_V changed linearly during pregnancy in the uterus or the chorioallantois. One-way ANOVAs with Tukey HSD *post-hoc* tests were used to determine differences in L_V, N_V and D_V between the VDE, the abembryonic side of the uterus, and the chorioallantois. Data were log-transformed to achieve normality for one-way ANOVAs. Lines with the highest R^2 values were selected to explain the relationship between the area of the chorioallantois and %TEDT, and the area of the VDE and %TEDT. Using bivariate correlations and Pearson's coefficients, we investigated potential relationships between the areas of the VDE and the chorioallantois.

RESULTS

Embryonic mass and metabolism

Wet and dry embryo mass was measured for 52 embryos from 34 *E. quoyii* females, and $\dot{V}_{O_2}$ was measured in 41 embryos from 29 females. Between stages 30 and 40, embryo wet mass increased from 0.07±0.01 g to 1.34±0.13 g, and dry mass increased from 0.003±0.001 g to 0.133±0.032 g. Embryonic $\dot{V}_{O_2}$ increased from 0.06±0.01 ml h^{-1} at stage 30 to 0.25±0.07 ml h^{-1} at stage 40.

Log–log transformation plots of %TEDT with embryo wet mass ($F_{1,31}$=323.68, P<0.0005, R^2=0.913; Fig. 2A), dry mass ($F_{1,31}$=328.19, P<0.0005, R^2=0.914) and $\dot{V}_{O_2}$ ($F_{1,26}$=168.69, P<0.0005, R^2=0.931; Fig. 2B) produced linear relationships. These plots verified that increases in embryo wet mass, dry mass and $\dot{V}_{O_2}$ during gestation are exponential.

The relationship between embryonic $\dot{V}_{O_2}$ and embryo wet (WM) and dry (DM) masses was significant: $\ln \dot{V}_{O_2} = 0.598 \cdot \ln \text{WM} = -1.433$ ($F_{1,26}$=153.86, P<0.0005, R^2=0.855; Fig. 2C); $\ln \dot{V}_{O_2} = 0.474 \cdot \ln \text{DM} = -0.303$ ($F_{1,26}$=201.58, P<0.0005, R^2=0.886; Fig. 2D).

Vasculature of the uterus

Immediately after ovulation and during early pregnancy, vasculature in the VDE appeared as a thick web of blood vessels and sinuses (Fig. 3A). Small invaginations in the blood vessel walls indicated that uterine angiogenesis occurs by intussusception. Small invaginations were indicative of trans-luminal pillars that expand and eventually split the vessel in two. Invaginations of the vessel walls were most abundant in females that were newly-ovulated and in the embryonic hemisphere of the uterus. Vessels in the VDE became more tortuous during pregnancy (Fig. 3B). There were visibly fewer invaginations of vessel walls on the abembryonic side of the uterus than in the VDE (Fig. 3C). Vessels

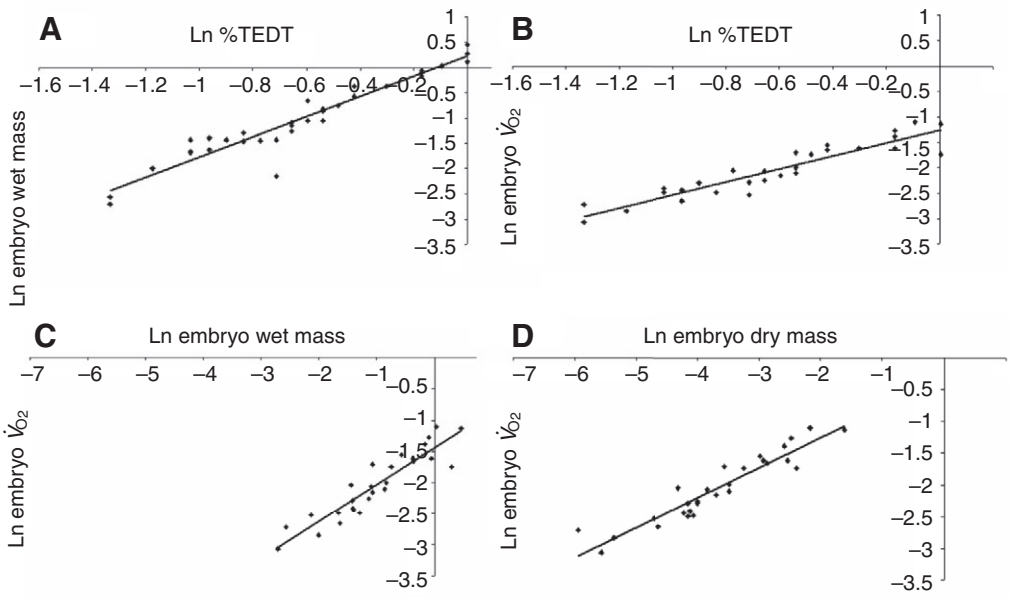

Fig. 2. (A) Natural log of embryo wet mass (g) as a function of the natural log of the percentage total embryonic development time (%TEDT) (R^2=0.913). (B) Natural log of embryo $\dot{V}_{O_2}$ (ml h^{-1}) as a function of the natural log of %TEDT (R^2=0.931). (C) Natural log of embryo $\dot{V}_{O_2}$ (ml h^{-1}) as a function of the natural log of embryo wet mass (g) (R^2=0.855). (D) Natural log of embryo $\dot{V}_{O_2}$ (ml h^{-1}) as a function of the natural log of embryo dry mass (g) (R^2=0.886). See text for linear regression statistics and equations.

in the abembryonic hemisphere also became more tortuous during pregnancy (Fig. 3D).

The VDE at the mesometrial pole of the uterus was visibly thicker and more opaque than the surrounding uterine tissue in uterine egg chambers of all 35 dissected pregnant females. The vasculature in the centre of the VDE was often discernible through the eyepiece of the confocal microscope, but the thickness of the uterine wall reduced the quality of *z*-stack images for analysis. Therefore, most images of the VDE used for analysis were taken close to the border of the VDE rather than the centre, but visual inspection of vessel density across the VDE suggested a uniform vasculature. A sudden and discernible decrease in vessel density distinguished the outer border of the VDE. Vessel density slowly decreased further from the VDE and closer to the abembryonic pole. The VDE was usually centered across the dorsal artery of the uterus but was noticeably skewed in specimens in which the embryo was oriented at an oblique angle to the dorsal surface of the uterus (Fig. 4).

L_V and N_V do not change during pregnancy in either the VDE or the abembryonic side of the uterus (Table 1). The average L_V during gestation was 67.5±1.7 mm per mm^2 in the VDE, and 30.6±0.9 mm per mm^2 on the abembryonic side of the uterus. Average N_V was 533.5±17.6 and 254.1±7.9 vessels per mm^2 in the VDE and the abembryonic side of the uterus, respectively. Vessel diameter, however, increased during pregnancy on the abembryonic side of the uterus but not in the VDE (Table 1). Average D_V in the VDE was 9.7±0.3 μm, whereas D_V on the abembryonic side of the uterus increased from 11.1±0.5 μm before stage 30 to 17.0±1.5 μm at stage 40.

Vasculature of the chorioallantois

Small invaginations in vessel walls of the chorioallantois indicated that angiogenesis occurs by intussusception in the chorioallantois, as it does in the uterus (Fig. 3E,F). Vessel-length density did not change during gestation in the chorioallantois (Table 1); the average chorioallantoic L_V was 78.2±2.3 mm per mm^2. Vessel density of the chorioallantois increased during gestation from 465.8±19.8 vessels per mm^2 at stage 32 to 575.0±29.1 vessels per mm^2 at stage 40 (Table 1). Chorioallantoic D_V decreased from 11.0±0.4 μm at stage 32 to 9.2±0.7 μm at stage 40 (Table 1).

The chorioallantois had a higher L_V and N_V than did both the VDE and the abembryonic side of the uterus (one-way ANOVA, Table 2), and the L_V and the N_V in the VDE were greater than those on the abembryonic side of the uterus (Table 2). Vessel diameter was the same in the chorioallantois and the VDE, but D_V was greatest on the abembryonic side of the uterus (Table 2).

Expansion of the vessel-dense ellipse (VDE) and the chorioallantois

Light microscopy of preserved eggs indicated that the chorioallantoic membrane is formed by stage 31. The area of both the chorioallantois and the VDE increased during gestation. The VDE was present in the uterus prior to the development of the chorioallantois, but the area of the chorioallantois began to exceed that of the VDE by stage 33. The chorioallantoic membrane covered a maximum of 80% of the egg at stage 40. The chorioallantois did not extend past the upper margin of the yolk sac during development, expanding only as the yolk sac became smaller.

A straight line best explained the relationship between the area of the chorioallantois and %TEDT ($F_{1,22}$=375.51, P<0.0005, R^2=0.945; Fig. 5A). Similarly, the relationship between %TEDT and the area of the VDE was also linear ($F_{1,33}$=111.91, P<0.0005, R^2=0.772; Fig. 5B). The area of the VDE correlated strongly with the area of the chorioallantois (r=0.840, P<0.0005).

Egg surface area increased during pregnancy ($F_{1,41}$=331.20, P<0.0005, R^2=0.890; Fig. 5C), causing the surrounding uterine egg chamber to stretch. The proportion of the uterine egg chamber covered by the VDE increased linearly during pregnancy ($F_{1,33}$=14.43, P=0.001, R^2=0.304; Fig. 5D). The proportion of the uterine egg chamber covered by the VDE correlated strongly with the proportion of the egg covered by the chorioallantois (r=0.585, P<0.003).

Uterine angiogenesis, embryonic growth and oxygen demand

The relationships between VDE area and embryo wet mass, and between VDE area and embryo $\dot{V}_{O_2}$, were not linear but exponential. The area of the VDE correlated strongly with both log-transformed embryo wet mass (r=0.788, P<0.0005) and log-transformed embryo $\dot{V}_{O_2}$ (r=0.863, P<0.0005).

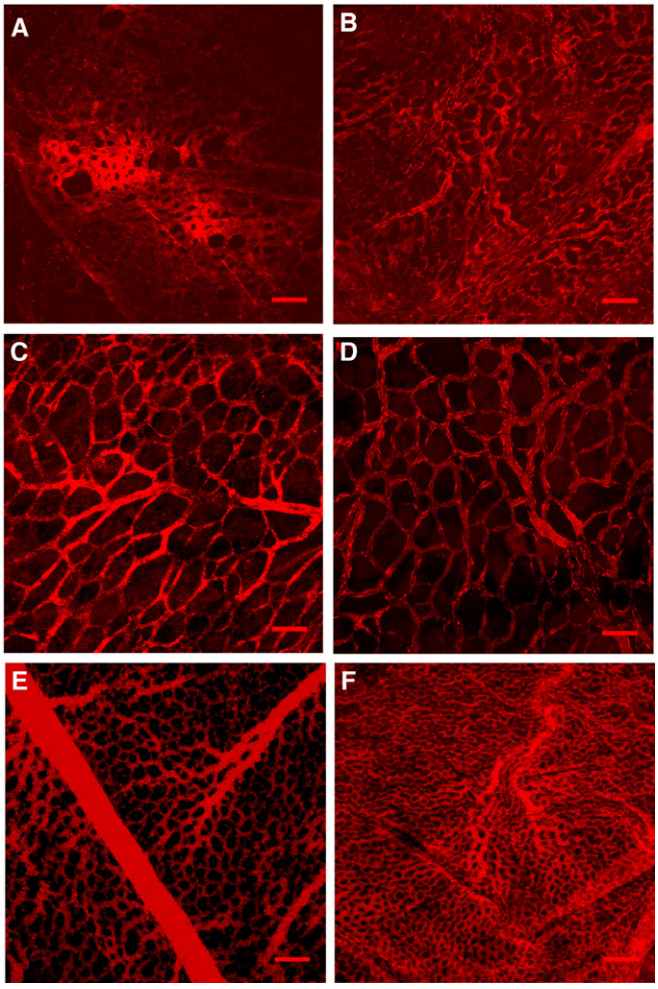

Fig. 3. Immunofluorescence confocal micrographs of uterine microvasculature of *Eulamprus quoyii*. Microvasculature from the embryonic hemisphere (A) and the abembryonic hemisphere (C) of *E. quoyii* uterus containing a stage 28 embryo. Microvasculature from the embryonic hemisphere (B) and the abembryonic hemisphere (D) of *E. quoyii* uterus containing a stage 40 embryo. Microvasculature from the chorioallantoic membrane of an *E. quoyii* embryo at stage 32.5 (E) and stage 40 (F). Bars: 100 μm.

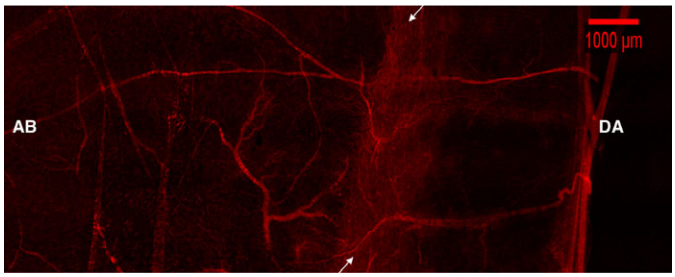

Fig. 4. Immunofluorescence confocal micrograph of uterine microvasculature of *E. quoyii*. The uterus is cut along the dorsal artery and longitudinally at the abembryonic pole (AB), and the tissue flattened onto a microscope slide. Several images, captured using a 10× lens and 900×900 μm fields of view, were pasted together using the tile scan function of the Zeiss LSM 510 Meta confocal microscope to create a composite image. A thick band of tissue (indicated by white arrows) forms the centre of the vessel-dense ellipse (VDE) in the embryonic hemisphere of the uterine egg chamber. The boundary of the VDE is not distinguishable at this magnification, but it lies approximately 2 mm to either side of the thick band of tissue. In most samples, the VDE is centered over the dorsal artery of the uterus. This uterine sample contained an embryo that was slightly rotated in the uterus, and the image shows that the VDE is now several millimeters to the left of the midline artery. DA, dorsal artery; AB, abembryonic side of the uterus.

DISCUSSION

A comparison of uterine and chorioallantoic angiogenesis in *E. quoyii* and *S. equalis*

Uterine angiogenesis occurs in concert with increasing embryonic mass and oxygen demand in *E. quoyii* and the only other species to have been studied, *S. equalis* (Parker et al., 2010a), but patterns of angiogenesis differ substantially between the two species.

In *S. equalis*, vessel density (N_V), vessel-length density (L_V) and vessel thickness (D_V) increase in both the embryonic and abembryonic hemispheres of the uterus during gestation (Fig. 6A). Furthermore, uterine N_V, L_V and D_V are greater in the embryonic hemisphere than the abembryonic hemisphere (Parker et al., 2010a) (Fig. 6A). The chorioallantois of *S. equalis* increases in size as the embryo develops, but exhibits no increase in N_V, L_V or D_V (Fig. 6A). By contrast, the uterine microvasculature in *E. quoyii* comprises a vessel-dense elliptical area (the VDE) directly opposite the embryo on the mesometrial side of the uterus; the VDE is not present in *S. equalis* (Fig. 6B). In *E. quoyii*, there is no change in N_V or L_V either in the VDE or on the abembryonic side of the uterus during pregnancy (Fig. 6B). Vessel diameter increases on the abembryonic side of the uterus (Fig. 6C,D) but does not change during pregnancy in the VDE. The VDE has higher N_V and L_V than the abembryonic side of the uterus (Fig. 6B), but abembryonic D_V exceeds D_V in the VDE. Vessel density increases and D_V decreases in the chorioallantois during gestation, whereas L_V does not change. The chorioallantois of *E. quoyii* not only becomes more vascular but also increases in size as the embryo develops.

In summary, the uterus of *S. equalis* becomes more densely vascularized per unit area during pregnancy and the chorioallantois expands but does not become more vascular. By contrast, uterine angiogenesis in *E. quoyii* manifests as an expansion of an already densely vascularized elliptical patch of tissue opposite the embryo, and the chorioallantois both expands and becomes more vascular (Fig. 6A). L_V in the embryonic hemisphere of the uterus of *S. equalis* reaches a maximum of 63.5±1.1 mm per mm^2 by the end of pregnancy (Parker et al., 2010a). However, L_V in the VDE of newly-ovulated *E. quoyii* (<stage 25) is already equal (65.7±7.1 mm per mm^2) to the maximum L_V reached in *S. equalis*. L_V (78.2±2.3 mm per mm^2) and N_V (575.0±29.1 vessels per mm^2) of the chorioallantois in stage 40 *E. quoyii* embryos exceeds chorioallantoic L_V and N_V in stage 40 *S. equalis* embryos (L_V, 47.5±1.0 mm per mm^2; N_V, 450±16.3 vessels per mm^2). Different patterns of uterine and chorioallantoic angiogenesis in *E. quoyii* and *S. equalis* suggest that the type or volume of placental exchange varies between the two species.

Angiogenesis on expanding surfaces

Substantial uterine stretching occurs during pregnancy (Fig. 5C), which must be taken into account when determining areas and rates of angiogenesis. For example, even though L_V and N_V in the VDE do not change during pregnancy, some angiogenesis must occur to prevent a decrease in these indices in a stretching uterus.

Table 1. Linear regressions of vessel length-density (L_V), vessel density (N_V) and vessel diameter (D_V) in the vessel-dense ellipse (VDE) of the uterus, on the abembryonic side of the uterus and in the chorioallantois of *E. quoyii*, as a function of total embryonic development time (%TEDT)

Area	Variable	Change during pregnancy	Result
VDE of uterus	L_V	No change	$F_{1,27}$=0.08, P=0.783, R^2=0.003
	N_V	No change	$F_{1,27}$=0.06, P=0.812, R^2=0.002
	D_V	No change	$F_{1,27}$=6.46, P=0.017, R^2=0.193
Abembryonic side of uterus	L_V	No change	$F_{1,29}$=2.16, P=0.152, R^2=0.069
	N_V	No change	$F_{1,29}$=3.66, P=0.066, R^2=0.112
	D_V	Increase	**$F_{1,29}$=32.12, P<0.0005, R^2=0.526**
Chorioallantois	L_V	No change	$F_{1,18}$=6.66, P=0.019, R^2=0.270
	N_V	Increase	**$F_{1,18}$=9.60, P=0.006, R^2=0.348**
	D_V	Decrease	**$F_{1,18}$=8.56, P=0.009, R^2=0.322**

P-values less than 0.017 are considered significant, due to a Bonferroni correction, and significant results are highlighted in bold.

Table 2. One-way ANOVAs of vessel length-density (L_V), vessel density (N_V) and vessel diameter (D_V) as a function of tissue region in *Eulamprus quoyii*

Variable	Result	Interpretation
L_V	$F_{2,77}$=316.29, P<0.0005	CA>VDE>abembryonic side of uterus
N_V	$F_{2,77}$=199.59, P<0.0005	CA>VDE>abembryonic side of uterus
D_V	$F_{2,77}$=18.85, P<0.0005	Abembryonic side of uterus>VDE=CA

VDE, vessel-dense region of the uterus; CA, chorioallantois.

We considered the possibility that expansion of the VDE might be an artefact of uterine stretching. If this were the case, the proportion of the uterine egg chamber covered by the VDE should remain the same during pregnancy, but the proportion increases linearly during pregnancy (Fig. 5D). Although stretching might contribute to some increase in the area of the VDE, it also actively grows and expands towards the abembryonic pole of the uterus.

What is the function of the VDE in *E. quoyii*?

The initial formation of the VDE is associated with the presence of the embryo rather than the development of the chorioallantois; the VDE is not yet formed in non-reproductive uteri but is evident in females containing newly-ovulated embryos (<stage 25) that do not yet have a chorioallantois. Once the chorioallantois has formed, the VDE and the chorioallantois grow in concert with each other, although the size of the chorioallantois quickly surpasses that of the VDE and remains larger than the VDE for the rest of pregnancy. For the majority of pregnancy, the VDE comprises only part of the uterine tissue that is in contact with the chorioallantois, and so forms only part of the chorioallantoic placenta. Further histological studies are needed to determine the cellular morphology of the VDE, but we suggest that the chorioallantoic placenta of *E. quoyii* is regionally diversified and that the original Type I classification for this species might need revision. The VDE is also not necessarily a structure that is specific to *E. quoyii* and we suggest that immunofluorescence confocal microscopy be used to reinvestigate lizards with already described placentae, as it is our experience that regional patterns of uterine vasculature are often difficult to detect using histological techniques.

Some VDEs were noticeably off-centre relative to the midline artery of the uterus in cases in which the embryo was at an oblique angle in the uterus (Fig. 5). We think this is compelling evidence that the VDE forms directly opposite the developing embryo,

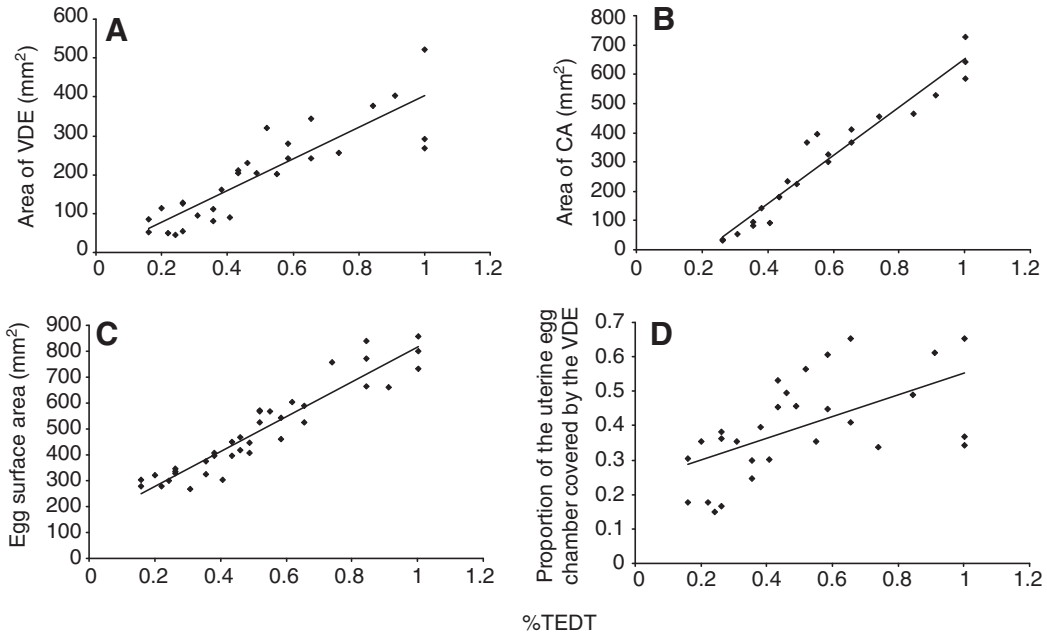

Fig. 5. (A) Area of the vessel-dense ellipse (VDE) as a function of percentage total embryonic development (%TEDT). (B) Area of the chorioallantois (CA) as a function of %TEDT. (C) Egg surface area as a function of %TEDT. (D) Proportion of the uterine egg chamber covered by the VDE as a function of %TEDT. See text for linear regression statistics.

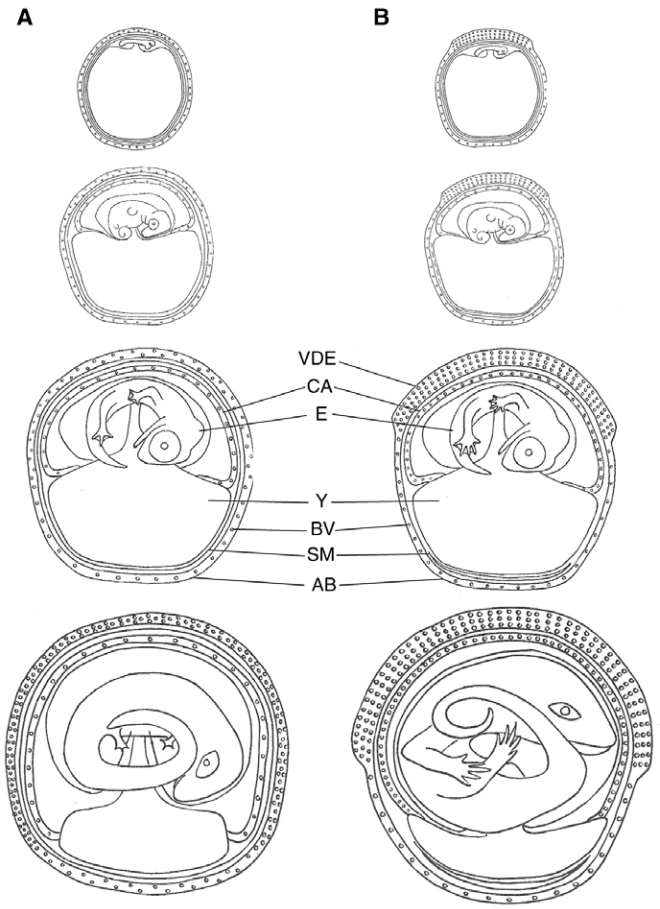

Fig. 6. Schematic diagrams of angiogenesis in the uterus and chorioallantois of *Saiphos equalis* (A) and *Eulamprus quoyii* (B). E, embryo; CA, chorioallantois; VDE, vessel-dense ellipse; BV, blood vessel; AB, abembryonic side of the uterus; SM, shell membrane; Y, yolk. The shell membrane in *E. quoyii* does not surround the egg in later embryonic stages but instead forms a fibrous pad underneath the yolk sac. Uterine angiogenesis in *S. equalis* occurs *via* vascularization of uterine tissue opposite the embryo and chorioallantois. The chorioallantois of *S. equalis* embryos increases in area but does not become more vascular during pregnancy. By contrast, thickened uterine tissue opposite of the embryo, called the VDE, is already highly vascular in early-stage *E. quoyii* embryos. The VDE does not become more vascular during pregnancy but does increase in area. The chorioallantois of *E. quoyii* embryos increases both in area and in vessel density.

presumably in response to signals from the embryo. The VDE then expands as the chorioallantois grows around the embryo, forming a site for physiological exchange. An already densely vascularized region that expands during pregnancy, instead of a larger region that becomes more densely vascularized, might be an evolutionary advantage, allowing more efficient exchanges between mother and embryo.

The question remains: what exactly is exchanged across this modified region of the chorioallantoic placenta? We initially thought that the VDE must be an area for the exchange of respiratory gases, as it is highly vascular and is opposite the chorioallantois, the major respiratory membrane of the embryo. A strong correlation between the area of the VDE and embryonic $\dot{V}_{O_2}$ also suggests that the VDE plays a role in respiratory exchange. Confusingly, our preliminary histology of this region indicates that the diffusion distance between the uterine blood vessels and the capillaries of the chorioallantois might be too big to facilitate efficient gas exchange; the blood vessels are not positioned close to the uterine epithelium, and the epithelial cells are columnar and not squamous.

Columnar uterine epithelial cells indicate that the VDE may have a secretory function, which is peculiar given that *E. quoyii* embryos are lecithotrophic. *Eulamprus quoyii* embryos contain adequate nutrients in the yolk to support development to completion, and it is possible to culture these embryos *in vitro*, albeit with very low success rates (Thompson, 1977). Furthermore, dry mass and organic mass of the whole egg decrease during gestation, indicating that there is no dependence on maternal sources for organic nutrition (Thompson, 1981). It is possible that the VDE could play a role in facultative placentotrophy (Stewart, 1989). Although embryos can survive without organic nutritional contributions from the uterus, pregnant *E. quoyii* transfer significant amounts of inorganic ions (Thompson, 1982) across the placenta to embryos, and have the capacity to transfer amino acids (Thompson, 1977). Further histology, and techniques such as enzyme histochemistry and immunohistochemistry, are required to determine whether the VDE has a respiratory or a secretory function.

It is likely that growth factors are among the signals exchanged between the VDE and chorioallantois, contributing to the angiogenesis in both of these tissues during pregnancy. An example of these growth factors is vascular endothelial growth factor (VEGF), the most potent of a suite of growth factors that initiates uterine angiogenesis in mammals (Ferrara and Davis-Smyth, 1997; Ferrara, 2004; Girling and Rogers, 2005). VEGF mRNA is upregulated in the uterus during pregnancy in *S. equalis* (Murphy et al., 2010), and might display similar patterns of expression in *E. quoyii*. Detailed descriptions of uterine angiogenesis in *S. equalis* (Parker et al., 2010a), and now in *E. quoyii*, provide the reference needed for future studies of uterine angiogenesis in lizards and of the mechanisms by which it occurs.

ACKNOWLEDGEMENTS

This research was funded by an Australian Research Council Discovery grant to M.B.T. and C.R.M. Animals were collected with New South Wales Scientific Collecting number S10693 and research was approved by the University of Sydney Animal Ethics Committee (number L04/9-2008/3/4883). We thank J. Herbert for assistance in dissections and respirometry, S. Clayman, K. Murphy, M. Murphy, D. Nelson and N. Pezaro for assistance in the field, and R. Andrews and M. Ramirez-Pinilla for valuable comments on the manuscript.

REFERENCES

Andrews, R. M. (2007). Effects of temperature on embryonic development of the veiled chameleon, *Chamaeleo calyptratus*. *Comp. Biochem. Physiol. A* **148**, 698-706.

Arany, Z., Foo, S.-Y., Ma, Y., Ruas, J. L., Bommi-Reddy, A., Girnun, G., Cooper, M., Laznik, D., Chinsomboon, J., Rangwala et al. (2008). HIF-independent regulation of VEGF and angiogenesis by the transcriptional coactivator PGC-1α. *Nature* **451**, 1008-1012.

Blackburn, D. G. and Vitt, L. J. (2002). Specializations of the chorioallantoic placenta in the Brazilian scincid lizard, *Mabuya heathi*: a new placental morphotype for reptiles. *J. Morphol.* **254**, 121-131.

Blackburn, D. G., Vitt, L. J. and Beuchat, C. A. (1984). Eutherian-like reproductive specializations in a viviparous reptile. *Proc. Natl. Acad. Sci. USA* **81**, 4860-4863.

DeMarco, V. (1993). Estimating egg retention times in sceloporine lizards. *J. Herpetol.* **27**, 453-458.

DeMarco, V. and Guillette, L. J., Jr (1992). Physiological cost of pregnancy in a viviparous lizard (*Sceloporus jarrovi*). *J. Exp. Zool.* **262**, 383-390.

Dufaure, J. P. and Hubert, J. (1961). Table de developpment du lizard vivipara: Lacerta (Zootoca) vivipara Jacquin. *Arch. Anat. Microsc. Morphol. Exp.* **50**, 309-328.

Fawcett, J. E. (1975). Effects of season, ovariectomy and hormone replacement therapy on the oviduct of *Anolis carolinensis* (Reptilia; Iguanidae). PhD Dissertation, University of Colorado.

Ferrara, N. (2004). Vascular endothelial growth factor: Basic science and clinical progress. *Endocr. Rev.* **25**, 581-611.

Ferrara, N. and Davis-Smyth, T. (1997). The biology of vascular endothelial growth factor. *Endocr. Rev.* **18**, 4-25.

Frye, F. L. (1973). *Husbandry, Medicine and Surgery in Captive Reptiles*. Bonner Springs, KS: VM Publishing Incorporated.

Girling, J. E. and Rogers, P. A. W. (2005). Recent advances in endometrial angiogenesis research. *Angiogenesis* **8**, 89-99.

Guillette, L. J. and Jones, R. E. (1985). Ovarian, oviductal and placental morphology of the reproductively bimodal lizard, *Sceloporus aeneus*. *J. Morphol.* **184**, 85-98.
Harris, J. W. and Stocker, H. (1998). *Handbook of Mathematics and Computational Science*, p. 107. New York: Springer-Verlag.
Hoyt, D. F., Vleck, D. and Vleck, C. M. (1976). Metabolism of avian embryos: ontogeny and temperature effects in the ostrich. *Condor* **80**, 265-271.
Masson, G. R. and Guillette, L. J. (1987). Changes in oviducal vascularity during the reproductive cycle of three oviparous lizards (*Eumeces obsoletus*, *Sceloporus undulates* and *Crotaphytus collaris*). *J. Reprod. Fertil.* **80**, 361-371.
Murphy, B. F., Belov, K. and Thompson, M. B. (2010). Evolution of viviparity and uterine angiogenesis: vascular endothelial growth factor (VEGF) in oviparous and viviparous skinks. *J. Exp. Zool. Mol. Dev. Evol.* **314**, 148-156.
Packard, G. C., Tracey, C. R. and Roth, J. J. (1977). The physiological ecology of reptilian eggs and embryos, and the evolution of viviparity within the class Reptilia. *Biol. Rev.* **52**, 71-105.
Parker, S. L. and Andrews, R. M. (2006). Evolution of viviparity in sceloporine lizards: in utero Po_2 as a developmental constraint during egg retention. *Physiol. Biochem. Zool.* **79**, 581-592.
Parker, S. L., Manconi, F., Murphy, C. R. and Thompson, M. B. (2010a). Uterine and placental angiogenesis in the Australian skinks, *Ctenotus taeniolatus* and *Saiphos equalis*. *Anat. Rec.* **293**, 829-838.
Parker, S. L., Murphy, C. R., and Thompson, M. B. (2010b). Uterine angiogenesis in squamate reptiles: Implications for the evolution of viviparity. *Herpetol. Conserv. Biol.* (In press).
Shine, R. (1983). Reptilian reproductive modes: the oviparity-viviparity continuum. *Herpetologica* **39**, 1-8.
Shine, R. (1985). The evolution of viviparity in reptiles: an ecological analysis. In *Biology of the Reptilia,* Vol 15 (ed. C. Gans and F. Billett), pp. 605-694. New York: John Wiley and Sons.
Stewart, J. R. (1989). Facultative placentotrophy and the evolution of squamate placentation: quality of eggs and neonates in *Virginia striatula*. *Am. Nat.* **133**, 111-137.
Thompson, J. (1977). The transfer of amino acids across the placenta of a viviparous lizard, *Sphenomorphus quoyii*. *Theriogenology* **8**, 158.
Thompson, J. (1981). A study of the sources of nutrients for embryonic development in a viviparous lizard, *Sphenomorphus quoyii*. *Comp. Biochem. Physiol. A* **70**, 509-518.
Thompson, J. (1982). Uptake of inorganic ions from the maternal circulation during development of the embryo of a viviparous lizard, *Sphenomorphus quoyii*. *Comp. Biochem. Physiol. A* **71**, 107-109.
Thompson, M. B. and Stewart, J. R. (1997). Embryonic metabolism and growth in lizards of the genus *Eumeces*. *Comp. Biochem. Physiol. A* **118**, 647-654.
Vitt, L. J. and Blackburn, D. G. (1991). Ecology and life history of the viviparous lizard *Mabuya bistrata* (Scincidae) in the Brazilian Amazon. *Copeia* **1991**, 916-927.
Vleck, D. (1987). Measurement of O_2 consumption, CO_2 production, and water vapour production in a closed system. *J. Appl. Physiol.* **62**, 2103-2106.
Weekes, H. C. (1927). Placentation and other phenomena in the scincid lizard *Lygosoma (Hinulia) quoyi*. *Proc. Linn. Soc.* **52**, 499-554.
Weekes, H. C. (1935). A review of placentation among reptiles with particular regard to the function and evolution of the placenta. *Proc. Zool. Soc. Lond.* **1935**, 625-645.
Yaron, Z. (1972). Effects of ovariectomy and steroid replacement on the genital tract of the viviparous lizard, *Xantusia vigilis*. *J. Morphol.* **136**, 313-326.